Ab Initio Prediction of Tryptophan Fluorescence Quenching by Protein Electric Field Enabled Electron Transfer

Patrik R. Callis,* Alexander Petrenko, Pedro L. Muiño,[†] and Jose R. Tusell

Department of Chemistry and Biochemistry, Montana State University, Bozeman, Montana 59717

Received: June 10, 2007; In Final Form: July 24, 2007

We report quantum mechanical−molecular mechanical (QM−MM) predictions of fluorescence quantum yields for 20 tryptophans in 17 proteins, whose yields span the range from 0.01 to 0.3, using ab initio computed coupling matrix elements for photoinduced electron transfer from the ^1L_a excited indole ring to a local backbone amide. The average coupling elements span the range $140-1000$ cm^{-1}, depending on tryptophan rotamer conformation. The matrix elements were from the singles configuration interaction matrix, and were largely insensitive to which of the three basis sets was used. Large fluctuations were seen on the time scale of tens of femtoseconds, caused primarily by side chain and backbone torsional variations for 150 ps of dynamics at 300 K. The largest coupling occurs for the chi1 $= -60°$ rotamer and is purely through-bond. There is no apparent correlation between the coupling magnitude and quantum yield, which is still dominated by energy gap and reorganization energy. The source of error bars for predicted quenching rates using the weak coupling golden rule may be due to inaccurate averaged Franck−Condon weighted densities because of inadequate simulation times and parameters and/or to failure of the weak coupled golden rule used in these predictions because of the broad distribution of Landau−Zener probabilities arising from the large variable coupling.

Introduction

The environment-sensitive intensity changes of tryptophan (Trp) fluorescence have been extensively used in the study of proteins for over four decades.[1,2] During most of that time, the underlying cause of the more than 30-fold range of fluorescence quantum yields observed for different single-Trp proteins remained a mystery. That is to say, even with a good X-ray structure in hand, no inkling of whether a given Trp in a protein would fluoresce strongly or weakly could be gleaned from the structural information. Aside from practical uses, the prediction of Trp fluorescence quantum yields and lifetimes represents a valuable, but somewhat unrealized, proving ground for testing theories of photoinduced electron transfer in proteins because of the relatively large number of measurements on systems with X-ray structures. Building on circumstantial evidence for electron transfer quenching by local amides contributed by many groups,[3−8] we have recently reported results of quantum mechanical−molecular mechanical (QM−MM) simulations on 24 Trp's in 17 proteins that led to a viable explanation and encouraging predictive power.[9,10] We found compelling correlation between the observed fluorescence quantum yields (lifetimes) and the energy and variance of the lowest charge transfer (CT) state described by transferring an electron from the ^1L_a excited indole ring[11] to the π^* molecular orbital (MO) localized on a local amide (an orbital that has been strongly implicated in low-energy electron capture mass spectrometry of peptides[12,13]). The extreme sensitivity to electrostatic environ-

ment of the CT state energy allows for electron transfer when fluctuations invert the CT−^1L_a state energy gap, followed by fast solvent relaxation about the CT state to create a low-lying, very weakly emitting solvent stabilized "radical ion pair".

A semiquantitative prediction based on the widely used Fermi golden rule expression[14,15]

$$k_{ET}(\Delta E_{00}) = \frac{2\pi}{\hbar}V^2\rho_{FC}(\Delta E_{00}) \tag{1}$$

for the electron transfer rate constant, k_{ET}, using only the average energy gap and variance was achieved with only two adjustable parameters: a universal electronic coupling constant, V, and a constant offset applied to the semiempirical zero-point transition energies, ΔE_{00}.[9] An ad hoc choice for the shape of the Franck−Condon (FC) weighted density of states function,[14] ρ_{FC}, led to a good fit for $V = 10$ cm^{-1} and an empirical shift of ΔE_{00} by -4000 cm^{-1} (physically unreasonable in retrospect). This method has been applied to the understanding of Trp fluorescence quantum yields in several additional cases.[16−19]

In this Letter, we report results of an ab initio method for computing V values. We find that the *average* ab initio values for a given protein are ∼20−90 times larger than the 10 cm^{-1} empirical fit value we used previously,[9] and that they exhibit rapid, large-amplitude fluctuations in response to small relative motions of the amide and indole during dynamics. The large average magnitude allows for a physically reasonable choice of ρ_{FC} which, when used in eq 1, retains semiquantitative agreement with experiment for Trp quantum yields in proteins. The large variability of V and CT state energies during molecular dynamics (MD) trajectories suggests that the electron transfer

* Corresponding author. Phone: 406-994-5414. Fax: 406-994-5407. E-mail: pcallis@montana.edu.
† Present address: Department of Chemistry, Mathematics and Physical Sciences, Saint Francis University, Loretto, PA 15940.
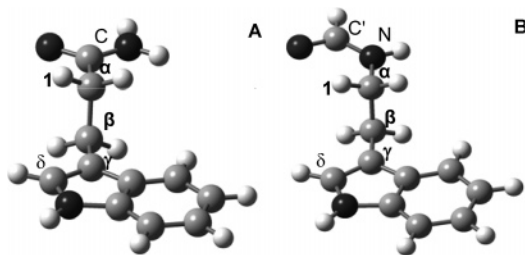
Figure 1. Model systems for closest tryptophan ring−backbone amide interactions, with key atoms labeled for defining dihedral angles: (A) model of tryptophan and C-terminal amide; (B) model of tryptophan and N-terminal amide. C = tryptophan amide carbonyl carbon; C′ = amide carbonyl carbon of preceding amino acid; N = tryptophan amide N; α = alpha carbon. Dihedral angles: chi1 = torsion about α−β, numbering from 1 to γ; chi2 = torsion about β−γ, numbering from α to δ; psi = torsion about α−C, numbering from 1 to N of the following amino acid.

kinetics will transiently span the range from the weak coupled (non-adiabatic) golden rule regime to the weak adiabatic regime,[14,20] depending on the details of local protein environment.

Methods

As before, the quantum yield is estimated with the expression $\Phi_f = k_r/(k_r + k_{nr} + k_i)$, where k_r and k_{nr} are the radiative and the non-electron-transfer non-radiative rate constants and k_i is the electron transfer rate constant for the ith protein. We use values found in aqueous solution: $k_r = 4 \times 10^7$ s^{-1} and $k_{nr} = 9 \times 10^7$ s^{-1}.[6] Instead of using a constant V value for all proteins, in this study

$$k_i = \frac{2\pi}{\hbar}\langle V_i^2 \rangle \langle \rho_i \rangle$$

where the $\langle V_i^2 \rangle$ average comes from 500 sets of coordinates generated during 150 ps QM−MM trajectories and the $\langle \rho_i \rangle$ average is from 15 000 points.

Molecular Systems. All results in this paper are for one of the two molecules shown in Figure 1. The geometry of these systems is precisely that obtained from MD trajectories for the proteins, except that only one amide is retained and capped with H atoms.

Matrix Elements. All ab initio electronic coupling elements were obtained using Gaussian 03, revision D.01.[21] Diabatic electronic matrix elements for V in eq 1 were taken from the singles configuration interaction (CIS) Hamiltonian matrix element coupling the highest occupied molecular orbital (HOMO) → ring π* lowest unoccupied molecular orbital (LUMO) and HOMO → amide π* MO configurations. We find that a CI basis consisting of only the three excitations from HOMO to LUMO + n (n = 0,1,2) adequately span the desired space for the systems studied here, because mixing of ring and amide MOs is not extensive. Subroutine MrgCIS in link 914 was slightly modified using the recommended link modification procedure,[21] so it will always write the CI ⟨AA,BB|AA,BB⟩ matrix, its eigenvalues, and its eigenvectors independent of other print options. The corresponding singlet and triplet adapted CI matrices were constructed from the output and were diagonalized to ensure that the results agreed with the normally printed singlet and triplet transition energies. The largest difficulty was the mixing between the amide π* and ring LUMO + 1 MOs and the corresponding mixing of the configurations involving these MOs. This problem was solved by determining which linear combination of the mixed MOs resulted in

TABLE 1: Average ab Initio Matrix Elements, $\langle |V_i| \rangle$, over 150 ps in cm^{-1} for Electron Transfer between the Indole Ring and C-Terminal Amide (Figure 1A)

	protein	STO-3G	3-21G	D95	Zindo[a]	QY[b]	chi1
1	dsb126	364(139)[c]	233(139)	262(137)	143(121)	0.013	180
2	cpl	320(170)	226(164)	217(163)	203(118)	0.025	+60
3	d6o	872(130)	710(225)	653(234)	275(97)	0.03	−60
4	sbc	265(130)	155(115)	252(154)	176(588)	0.03	180
5	trpcage1	251(132)	172(131)	235(158)	223(120)	0.03	180
6	bpp	911(168)	731(247)	628(249)	265(115)	0.031	−60
7	nscp	170(115)	152(110)	160(113)	306(134)	0.033	180
8	lyd138	213(123)	144(111)	186(139)	114(88)	0.044	180
9	lyd126	839(194)	640(268)	547(269)	237(96)	0.06	−60
10	ctx	233(133)	197(129)	237(149)	217(135)	0.1	+60
11	mlt	296(145)	161(118)	284(154)	175(110)	0.115	180
12	gcn	343(174)	259(168)	361(190)	122(2?85)	0.12	180
13	barn71	976(102)	882(171)	799(171)	230(84)	0.122	−60
14	b8r	262(137)	184(129)	218(140)	205(141)	0.13	180
15	barn35	166(131)	154(112)	137(106)	247(128)	0.142	180
16	dsb76	284(132)	196(128)	245(141)	101(88)	0.2	180
17	stn	896(136)	748(220)	652(223)	177(48)	0.29	−60
18	azb	527(154)	237(163)	296(172)	145(102)	0.31	180
19	rnt	513(152)	278(170)	341(157)	213(108)	0.31	180
20	pfk	985(93)	894(143)	870(149)	255(100)	0.35	−60

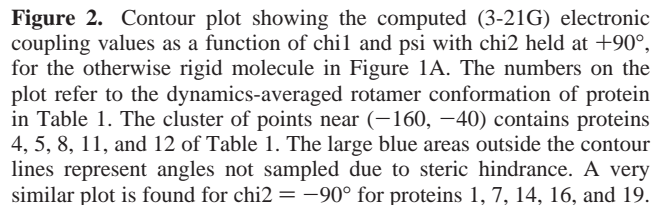[a] INDO/S-CIS. [b] Experimental fluorescence quantum yield. [c] In parentheses signifies 1 standard deviation.

maximum amide π* density; this linear combination of CI matrix elements then gave the desired interaction element. Three basis sets were compared: STO-3G, 3-21G, and the Dunning/ Huzinga full double-ζ basis, D95.[22]

Density of States. Even with large atomic orbital (AO) and CI bases, CIS energies are too crude to provide reasonable estimates of energy gaps. For that, we have relied, as before, on Zerner's INDO/S-CIS (Zindo).[23] The trajectories were conducted with the QM bond lengths fixed using the SHAKE routine at values representative of the CT state. CASPT2[24,25] calculations for several formamide−indole pairs show that the ^1L_a state energy increases by ∼4000 cm^{-1} relative to that of CT as the geometry is increased from that at the ^1L_a energy minimum to that of the CT state minimum.[26] In addition, CASPT2 CT state energies are found to be 1000−3000 cm^{-1} higher that those estimated using Zindo.[26] Therefore, it is expected that Zindo-computed ΔE_{00} values computed at the CT geometry should be increased by about 5000 ± 1000 cm^{-1} to make a realistic estimate of the true ΔE_{00}.

MD Simulations. Charmm[27] was used as in previous work[9] except that version 31b1 was used instead of 26b2, the length of the simulations was 150 ps instead of 50 ps, and the proteins were typically solvated in 40 Å radius spheres of TIP3 explicit water instead of 30 Å radius spheres.

Results and Discussion

Table 1 compares the average calculated $\langle |V_i| \rangle$ for electron transfer to the C-terminal amide (Figure 1A) using three different basis sets and the semiempirical values for 20 of the 24 Trp's for which predictions were made previously.[9,28] It is seen that the average ab initio values fall in the range 140−1000 cm^{-1}, with dependence on protein that is fairly insensitive to basis set. Insensitivity to basis set has been noted previously.[29,30] The semiempirical values, in contrast, show a smaller range and are not correlated with the ab initio values. Significantly, there is no correlation of $\langle |V_i| \rangle$ with the experimental quantum yields in any case. This result is consistent with our previous assumption that V is not the rate determining parameter for amide quenching of Trp fluorescence because of the large inherent energy gap (small averaged FC densities) except when the protein environment provides a sufficiently stabilizing

Letters

J. Phys. Chem. B, Vol. 111, No. 35, 2007 **10337**

Figure 2. Contour plot showing the computed (3-21G) electronic coupling values as a function of chi1 and psi with chi2 held at $+90°$, for the otherwise rigid molecule in Figure 1A. The numbers on the plot refer to the dynamics-averaged rotamer conformation of protein in Table 1. The cluster of points near $(-160, -40)$ contains proteins 4, 5, 8, 11, and 12 of Table 1. The large blue areas outside the contour lines represent angles not sampled due to steric hindrance. A very similar plot is found for chi2 $= -90°$ for proteins 1, 7, 14, 16, and 19.

electric potential difference to create transient resonance between the fluorescing and CT states.

$\langle|V_i|\rangle$ values using the STO-3G basis for the N-terminal amide (Figure 1B) are slightly smaller, falling in the range 120–500 cm^{-1}.

The large ab initio and semiempirical magnitudes found in the present work for coupling through methylene bridges could have been anticipated from a number of studies.[30-34] As an independent check on our results, we applied the method of avoided crossing,[35-37] finding quite similar numbers in the cases examined.

We have established that the main source of fluctuation in V during dynamics simulations is due to large non-Condon behavior from strong dependence on torsional angles. Similar dependence on orientation of through-bond and through-space interaction has been observed in several studies.[29,31,38,39] Table 1 includes the one variable that does appear to correlate well with $\langle|V_i|\rangle$, the dihedral angle chi1. Uniformly, $\langle|V_i|\rangle$ is much larger and the relative standard deviation (amplitude of fluctuations) is smaller for those proteins for which chi1 is nominally near $-60°$, a conformation which is close to that in Figure 1A. Calculations done for the space-separated amide and indole ring for chi1 near $-60°$, with the atoms in identical positions, show only a small interaction (0–25 cm^{-1}), which means that this large interaction is virtually all through-bond for the $-60°$ conformation. When chi1 is nominally $+60$ or $180°$, $\langle|V_i|\rangle$ is always found to be $\sim$4 times smaller, and fluctuations often reduce instantaneous values to <5 cm^{-1}. In these conformations, direct (through-space) interactions most likely exhibit quantum mechanical interference with the through-bond component. Such interference is extremely sensitive to the relative orientation of the ring and amide groups, and has recently been implicated in long-range electron transfer through proteins.[40,41]

The above conclusions are largely based on contour plots such as the one shown in Figure 2, displaying computed (RHF/3-21G) V values as a function of *only* chi1 and psi torsions while holding chi2 at $+90°$. The numbers on the plot refer to the dynamics-averaged rotamer conformation of the proteins in Table 1. It is seen that broad maxima occur when chi1 $= \sim -60°$ and psi $= \sim -40$ or $+140°$ and that all proteins studied here have psi values either near -40 or $+140°$. These positions happen to maximize the through-bond "π conjugation" between the amide and indole ring. When psi is near -130 or $+50°$, the

Figure 3. Franck–Condon density curves used in eq 1 for electron attachment to the amide (curve a, dash–dot), ionization of indole with $\Delta E_{00} = -4000$ cm^{-1} (curve b, dots), ionization of indole with $\Delta E_{00} = 0$ (curve c, dashed), and ionization of indole with $\Delta E_{00} = +4500$ cm^{-1} (curve d, solid).

amide carbon π AO is perpendicular to the direction of the π AOs of the ring LUMO. For chi1 $= \sim +60$ and $180°$, V is seen to be uniformly small and in regions for which V will vary rapidly with small changes in chi1 and psi, as seen in MD trajectories.

Figure 3 speaks to the Franck–Condon weighted density of states, and the issue of empirical correction of Zindo energies. We model ρ_{FC} as the overlap integral of FC densities for the electron detachment from an indole ring (curves b–d) in Figure 3 and the electron attachment to formamide (curve a in Figure 3).[9] Curves b–d represent $\Delta E_{00} = -4000$, 0, and $+4500$ cm^{-1}, respectively. These three cases lead to $\rho_{FC} = 9 \times 10^{-5}, 1 \times 10^{-5}$, and 9×10^{-8} (cm^{-1})$^{-1}$, respectively. With our earlier ad hoc fit of the experimental data, the use of $|V| = 10$ cm^{-1} required *subtracting* 4000 cm^{-1} from the ΔE_{00} values obtained from the QM–MM trajectories (curve b), whereas with the present scheme ($\langle|V_i|\rangle = 140-1000$ cm^{-1}) the best fit is obtained by *adding* 4500–5000 cm^{-1} (similar to curve d), values that are consistent with expectations from CASPT2 calculations.

Figure 4 shows an example of fitting predicted and experimental quantum yields using the "ab initio" scheme presented above. The larger V values tend to exaggerate the lack of precision for those proteins with quantum yields in the intermediate range. Nevertheless, if dsb76 and pfk are excluded (as was done previously[9]), the linear fit has a correlation coefficient of 0.80 compared to 0.90 found previously.[9] At least two general reasons can be identified as possible causes for the imprecision. It is possible that even 150 ps trajectories do not capture the relevant configuration space. Single molecule experiments on the quenching of flavin fluorescence in proteins suggest this possibility.[42] Another possibility is that the large V values lead to breakdown of the golden rule. Indeed, preliminary estimation of the Laudau–Zener curve crossing probabilities suggest that the weak adiabatic regime[20] is more relevant for some of the proteins.

The use of CIS diabatic interaction elements is one of several techniques that have been accepted as providing reasonable values in estimating ET rates.[29,31,43] Given the modest ET rates considered in typical Trp quenching ($< 1 \times 10^{10}$ s^{-1}), it is clear that the system spends considerable time (> 100 ps) prior to an ET event following excitation. This means that initial state preparation becomes an issue. Given the large values and rapid fluctuations of V found in the present work, one anticipates a spectrum of pathways that lead to quenching through the CT
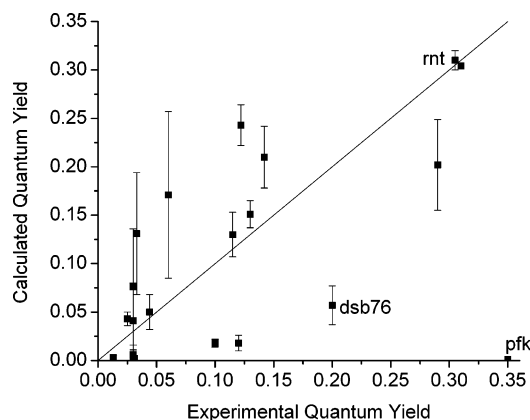
Figure 4. Representative plot of calculated vs experimental fluorescence quantum yields for 20 Trp's in 17 proteins using the D95 ab initio $\langle V_i^2 \rangle$ values and the new Franck–Condon density of states scheme described in the text. The error bars are the standard deviations for three 50 ps MD trajectories. Here, 4700 cm^{-1} is added to the Zindo CT energy computed at CT geometry, and a Gaussian with standard deviation = 3000 cm^{-1} is used for the amide electron attachment FC density spectrum (see Figure 3). For the buried Trp 59 of rnt only, the quantum yield was computed from the small equilibrium constant (positive ΔG_0) for the electron transfer process stemming from its small reorganization energy (the relaxed CT state lies above the ^1L_a state). For dsb76 and pfk, the present accuracy of our ΔG_0 estimates leaves open the possibility that equilibrium will favor the ^1L_a state, and the quantum yield predictions will be much higher.

state. It is commonly accepted that the excited state is created in a time short relative to nuclear motion time scales. Immediately following excitation, the wavefunction will be localized on the indole ring, and the diabatic interaction elements presented here should be valid for use in the Fermi golden rule for those systems in resonance at the instant of excitation. From the small FC factors consistent with the large $\langle |V_i| \rangle$ values, the vast majority of cases will, however, not find the system in resonance at the moment of excitation, and the system will have relaxed electronically and vibrationally to the thermalized zero point of the ^1L_a electronic eigenstate. This will contain a CT component determined by its energy and interaction relative to the CT state. In principle, if resonance is approached slowly enough and V is changing slowly, the adiabatic limit will prevail during the avoided crossing with the CT state. Quenching depends on whether the solvent near the adiabatically forming CT state is poised for inertial relaxation ($\sim$50 fs) or not. If the solvent relaxation does not trap the CT state, recrossing to the ^1L_a state is likely. MD simulations suggest, however, that both the energy gap and the interaction often change drastically in 10 fs but that they are not correlated. This time scale borders on the dephasing time associated with electronic excitation. Conceivably, rapid changes in either the gap or interaction will create an electronic state sufficiently non-stationary that the non-adiabatic regime is reached. The picture that emerges points to a continuum of possibilities for an individual excited Trp, ranging from the limits of purely non-adiabatic (fast change in energy gap and small V) to purely adiabatic (slow energy gap change and large V), with many cases falling into an intermediate behavior. Ratner and co-workers have recently presented an illuminating discussion of these issues.[44,45] We are presently investigating schemes in which charge densities are updated on the 1 fs time scale in our QM–MM simulations to identify adiabatic behavior and to estimate transmission coefficients.

References and Notes

(1) Eftink, M. R. *Methods Biochem. Anal.* **1991**, *35*, 127–205.
(2) Lakowicz, J. *Principles of Fluorescence Spectroscopy*, 2nd ed; Plenum: New York, 1999.
(3) Cowgill, R. W. *Arch. Biochem. Biophys.* **1963**, *100*, 36–44.
(4) Feitelson, J. *Isr. J. Chem.* **1970**, *8*, 241–252.
(5) Petrich, J. W.; Chang, M. C.; McDonald, D. B.; Fleming, G. R. *J. Am. Chem. Soc.* **1983**, *105*, 3824–3832.
(6) Chen, Y.; Barkley, M. D. *Biochemistry* **1998**, *37*, 9976–9982.
(7) Supkowski, R. M.; Bolender, J. P.; Smith, W. D.; Reynolds, L. E. L.; Horrocks, W. D. *Coord. Chem. Rev.* **1999**, *185*, 307–319.
(8) Sillen, A.; Hennecke, J.; Roethlisberger, D.; Glockshuber, R.; Engelborghs, Y. *Proteins: Struct., Funct., Genet.* **1999**, *37*, 253–263.
(9) Callis, P. R.; Liu, T. *J. Phys. Chem. B* **2004**, *108*, 4248–4259.
(10) Callis, P. R.; Vivian, J. T. *Chem. Phys. Lett.* **2003**, *369*, 409–414.
(11) Broos, J.; Tveen-Jensen, K.; de Waal, E.; Hesp, B. H.; Callis, P. R.; Canters, G. W.; Jackson, B. J. *Angew. Chem. Int. Ed.*, in press.
(12) Sobczyk, M.; Anusiewicz, W.; Berdys-Kochanska, J.; Sawicka, A.; Skurski, P.; Simons, J. *J. Phys. Chem. A* **2005**, *109*, 250–258.
(13) Anusiewicz, I.; Sobczyk, M.; Berdys-Kochanska, J.; Skurski, P.; Simons, J. *J. Phys. Chem. A* **2005**, *109*, 484–492.
(14) Bixon, M.; Jortner, J. *Adv. Chem. Phys.* **1999**, *106*, 35–202.
(15) Kestner, N. R.; Logan, J.; Jortner, J. *J. Phys. Chem.* **1974**, *78*, 2148–2166.
(16) Kurz, L. C.; Fite, B.; Jean, J.; Park, J.; Erpelding, T.; Callis, P. *Biochemistry* **2005**, *44*, 1394–1413.
(17) Chen, J. J.; Flaugh, S. L.; Callis, P. R.; King, J. *Biochemistry* **2006**, *45*, 11552–11563.
(18) Xu, J. H.; Toptygin, D.; Graver, K. J.; Albertini, R. A.; Savtchenko, R. S.; Meadow, N. D.; Roseman, S.; Callis, P. R.; Brand, L.; Knutson, J. R. *J. Am. Chem. Soc.* **2006**, *128*, 1214–1221.
(19) Liu, T.; Callis, P. R.; Hesp, B. H.; de Groot, M.; Buma, W. J.; Broos, J. *J. Am. Chem. Soc.* **2005**, *127*, 4104–4113.
(20) Hynes, J. T. *J. Phys. Chem.* **1986**, *90*, 3701–3706.
(21) Frisch, M. J.; Trucks, G. W.; Schlegel, H. B.; Scuseria, G. E.; Robb, M. A.; Cheeseman, J. R.; Montgomery, J. A.; Vreven, T.; Kudin, K. N.; Burant, J. C.; Millam, J. M.; Iyengar, S. S.; Tomasi, J.; Barone, V.; Mennucci, B.; Cossi, M.; Scalmani, G.; Rega, N.; Petersson, G. A.; Nakatsuji, H.; Hada, M.; Ehara, M.; Toyota, K.; Fukuda, R.; Hasegawa, J.; Ishida, M.; Nakajima, T.; Honda, Y.; Kitao, O.; Nakai, H.; Klene, M.; Li, X.; Knox, J. E.; Hratchian, H. P.; Cross, J. B.; Bakken, V.; Adamo, C.; Jaramillo, J.; Gomperts, R.; Stratmann, R. E.; Yazyev, O.; Austin, A. J.; Cammi, R.; Pomelli, C.; Ochterski, J. W.; Ayala, P. Y.; Morokuma, K.; Voth, G. A.; Salvador, P.; Dannenberg, J. J.; Zakrzewski, V. G.; Dapprich, S.; Daniels, A. D.; Strain, M. C.; Farkas, O.; Malick, D. K.; Rabuck, A. D.; Raghavachari, K.; Foresman, J. B.; Ortiz, J. V.; Cui, Q.; Baboul, A. G.; Clifford, S.; Cioslowski, J.; Stefanov, B. B.; Liu, G.; Liashenko, A.; Piskorz, P.; Komaromi, I.; Martin, R. L.; Fox, D. J.; Keith, T.; Al-Laham, M. A.; Peng, C. Y.; Nanayakkara, A.; Challacombe, M.; Gill, P. M. W.; Johnson, B.; Chen, W.; Wong, M. W.; Gonzalez, C.; Pople, J. A. *Gaussian 03*, revision D.01; Gaussian, Inc.: Wallingford, CT, 2004.
(22) Dunning, T. H.; Hay, P. J. In *Modern Theoretical Chemistry*; Schaefer, H. F., III, Ed.; Plenum: New York, 1976; Vol. 3, pp 1–28.
(23) Ridley, J.; Zerner, M. *Theor. Chim. Acta* **1973**, *32*, 111–134.
(24) Andersson, K.; Malmqvist, P.-Å.; Roos, B. O.; Sadlej, A. J.; Wolinski, K. *J. Phys. Chem.* **1990**, *94*, 5483–5488.
(25) Andersson, K.; Barysz, M.; Bernhardsson, A.; Blomberg, M. R. A.; Cooper, D. L.; Fülscher, M. P.; de Graaf, C.; Hess, B. A.; Karlström, G.; Lindh, R.; Malmqvist, P.-Å.; Nakajima, T.; Neogrády, P.; Olsen, J.; Roos, B. O.; Schimmelpfennig, B.; Schütz, M.; Seijo, L.; Serrano-Andrés, L.; Siegbahn, P. E. M.; Stålring, J.; Thorsteinsson, T.; Veryazov, V.; Widmark, P.-O. *MOLCAS5.4*; Lund University: Sweden, 2000.
(26) Liu, T.; Callis, P. R. Unpublished work, 2005.
(27) MacKerell, A. D. Bashford, D.; Bellott, M.; Dunbrack, R. L.; Evanseck, J. D.; Field, M. J.; Fischer, S.; Gao, J.; Ha, S.; Joseph-McCarthy, D.; Kuchnir, L.; Kuczera, K.; Lau, F. T. K.; Mattos, C.; Michnick, S.; Ngo, T.; Nguyen, D. T.; Prodhom, B.; Reiher, W. E., III; Roux, B.; Schlenkrich, M.; Smith, J. C.; Stote, R.; Straub, J.; Watanabe, M.; Wiorkiewicz-Kuczera, J.; Yin, D.; Karplus, M., Jr. *J. Phys. Chem. B* **1998**, *102*, 3586–3616.
(28) Two of these involved acceptors that were not the local backbone amides considered in this work. The other two were were Trp 94 of barnase at neutral pH and Trp 126 of the double mutant dsb Q24A/N127A, both of which gave excellent agreement with experiment previously.
(29) Zhang, L. Y.; Friesner, R. A.; Murphy, R. B. *J. Chem. Phys.* **1997**, *107*, 450–459.
(30) Liang, C. X.; Newton, M. D. *J. Phys. Chem.* **1993**, *97*, 3199–3211.
(31) Toutounji, M. M.; Ratner, M. A. *J. Phys. Chem. A* **2000**, *104*, 8566–8569.
(32) Paddon-Row, M. N.; Shephard, M. J.; Jordan, K. D. *J. Phys. Chem.* **1993**, *97*, 1743–1745.

Letters

J. Phys. Chem. B, Vol. 111, No. 35, 2007 **10339**

(33) Liu, Y. P.; Newton, M. D. *J. Phys. Chem.* **1995**, *99*, 12382−12386.

(34) Amini, A.; Harriman, A. *J. Phys. Chem. A* **2004**, *108*, 1242−1249.

(35) Gao, Y. Q.; Marcus, R. A. *J. Phys. Chem. A* **2002**, *106*, 1956−1960.

(36) Amini, A.; Harriman, A. *J. Photochem. Photobiol., C* **2003**, *4*, 155−177.

(37) Amini, A.; Harriman, A. *Phys. Chem. Chem. Phys.* **2003**, *5*, 4556−4562.

(38) Daizadeh, I.; Medvedev, E. S.; Stuchebrukhov, A. A. *Proc. Natl. Acad. Sci. U.S.A.* **1997**, *94*, 3703−3708.

(39) Mikkelsen, K. V.; Ratner, M. A. *J. Phys. Chem. A* **1989**, *93*, 1759−1770.

(40) Prytkova, T. R.; Kurnikov, I. V.; Beratan, D. N. *Science* **2007**, *315*, 622−625.

(41) Onuchic, J. N.; Kobayashi, C.; Miyashita, O.; Jennings, P.; Baldridge, K. K. *Philos. Trans. R. Soc. London, Ser. B* **2006**, *361*, 1439−1443.

(42) Yang, H.; Luo, G. B.; Karnchanaphanurach, P.; Louie, T. M.; Rech, I.; Cova, S.; Xun, L. Y.; Xie, X. S. *Science* **2003**, *302*, 262−266.

(43) Newton, M. D. *Chem. Rev.* **1991**, *91*, 767−792.

(44) Ashkenazi, G.; Kosloff, R.; Ratner, M. A. *J. Am. Chem. Soc.* **1999**, *121*, 3386−3395.

(45) Kosloff, R.; Ratner, M. A. *J. Phys. Chem. B* **2002**, *106*, 8479−8483.